

This is the accepted manuscript made available via CHORUS. The article has been published as:

Magnetospheric Multiscale Observations of the Electron Diffusion Region of Large Guide Field Magnetic Reconnection

S. Eriksson *et al.*

Phys. Rev. Lett. **117**, 015001 — Published 1 July 2016

DOI: [10.1103/PhysRevLett.117.015001](https://doi.org/10.1103/PhysRevLett.117.015001)

Magnetospheric Multiscale Observations of the Electron Diffusion Region of Large Guide Field Magnetic Reconnection

S. Eriksson¹, F. D. Wilder¹, R. E. Ergun^{1,2}, S. J. Schwartz^{1,3}, P. A. Cassak⁴, J. L. Burch⁵, L.-J. Chen⁶, R. B. Torbert^{5,7}, T. D. Phan⁸, B. Lavraud^{9,10}, K. A. Goodrich^{1,2}, J. C. Holmes^{1,2}, J. E. Stawarz^{1,2}, A. P. Sturmer^{1,2}, D. M. Malaspina¹, M. E. Usanova¹, K. J. Trattner¹, R. J. Strangeway¹¹, C. T. Russell¹¹, C. J. Pollock¹², B. L. Giles¹², M. Hesse¹², P.-A. Lindqvist¹³, J. Drake⁶, M. A. Shay¹⁴, R. Nakamura¹⁵, and G. T. Marklund¹³

¹ Laboratory of Atmospheric and Space Sciences, University of Colorado, Boulder, Colorado, 80303, USA

² Department of Astrophysical and Planetary Sciences, University of Colorado, Boulder, Colorado, 80303, USA

³ The Blackett Laboratory, Imperial College, London, United Kingdom

⁴ West Virginia University, Morgantown, West Virginia, USA

⁵ Southwest Research Institute, San Antonio TX, USA

⁶ University of Maryland, College Park, Maryland, USA

⁷ University of New Hampshire, Durham, New Hampshire, USA

⁸ Space Sciences Laboratory, University of California, Berkeley, California, USA

⁹ Institut de Recherche en Astrophysique et Planétologie, Université de Toulouse, France

¹⁰ Centre National de la Recherche Scientifique, UMR 5277, Toulouse, France

¹¹ University of California, Los Angeles, Los Angeles, California, USA

¹² NASA, Goddard Space Flight Center, Greenbelt, Maryland, USA

¹³ KTH Royal Institute of Technology, Stockholm, Sweden

¹⁴ University of Delaware, Newark, Delaware, USA

¹⁵ Space Research Institute, Austrian Academy of Sciences, Graz, Austria

ABSTRACT

We report observations from the Magnetospheric Multiscale (MMS) satellites of a large guide field magnetic reconnection event. The observations suggest that two of the four MMS spacecraft sampled the electron diffusion region whereas the other two spacecraft detected the exhaust jet from the event. The guide magnetic field amplitude is approximately four times that of the reconnecting field. The event is accompanied by a significant parallel electric field (E_{\parallel}) that is larger than predicted by simulations. The high-speed (~ 300 km/s) crossing of the electron diffusion region limited the data set to one complete electron distribution inside of the electron diffusion region, which shows significant parallel heating. The data suggest that E_{\parallel} is balanced by a combination of electron inertia and a parallel gradient of the gyrotropic electron pressure.

I. INTRODUCTION

Magnetic reconnection is a universal plasma process that can change the topological configuration of a magnetic field (\mathbf{B}) and, in the process, converts magnetic energy into kinetic energy and heat. It is known to dramatically impact behavior in heliospheric [1-8], astrophysical [e.g., 9], and laboratory plasmas [e.g., 10]. Great progress has been made in the past few decades in understanding magnetic reconnection at the ion scale [11, and references therein], but the physics of the electron scale is not fully understood, particularly in collisionless plasmas [12,13]. The Magnetospheric Multiscale (MMS) mission is designed to study electron-scale ($\lambda_e = c/\omega_{pe}$, the electron skin depth, where $\omega_{pe}^2 = N_e e^2 / m_e \epsilon_0$) physics of magnetic reconnection [14].

The first phase of the MMS mission studies the sub-solar magnetopause [14]. In this region, the shocked solar wind plasma, called the magnetosheath, carries the interplanetary magnetic field to the boundary of the Earth's magnetosphere where it can reconnect with the geomagnetic field. Reconnection under these conditions is highly asymmetric [e.g., 15, 16], with the magnetosheath density being on the order of ten times the density in the magnetosphere.

The MMS spacecraft encountered the electron diffusion region (EDR) of a magnetic reconnection event [17]. The reported event was nearly anti-parallel; the magnetic field component out of the reconnection plane, the guide field, was small compared to the reconnecting magnetic field. The reconnecting parallel electric field (E_{\parallel}) in this region was small, ~ 3 mV/m as expected, and was accompanied by an agyrotropic electron distribution that results from the mixing of magnetosheath and magnetosphere plasma [13,15,16].

In this letter, we present MMS observations that suggest an EDR crossing in which the guide field is approximately 4 times larger than the reconnecting field. These are the first strong guide field EDR observations by MMS. In the case of a large guide field, electrons can remain magnetized, even in the EDR [e.g. 18-21]. Recent simulations of asymmetric reconnection with equal guide and reconnecting fields found that electron agyrotropy could still occur in the EDR if magnetic field gradient scale lengths (typically on the order of λ_e) are as small as the electron gyroradius ($\rho_e = V_{e\perp}/\Omega_e$) [18]. Predicted E_{\parallel} amplitudes are on the order of 3-4 mV/m.

In MMS observations of large guide field reconnection, $|E_{\parallel}|$ reaches amplitudes of ~ 15 mV/m, which is four to five times the expected amplitude. The observations show strongly enhanced dissipation ($\mathbf{J} \cdot (\mathbf{E} + \mathbf{V}_e \times \mathbf{B}) > 0$) and significant heating of electrons parallel \mathbf{B} . We show evidence of electrons accelerated by the parallel electric field in the EDR, and find no evidence of agyrotropy, as expected since ρ_e (~ 0.4 km) $<$ λ_e (~ 1.7 km). These results suggest that in the large guide field limit, the electron pressure gradient parallel to \mathbf{B} and/or electron inertial term of the generalized Ohm's law may balance E_{\parallel} .

II. OBSERVATIONS

Figure (1) shows data from MMS3, which credibly encountered the EDR. The horizontal axis covers 6 s. The location of MMS3 (at the top of the figure) is near the dusk flank of the Earth's magnetopause. This event was previously discussed as evidence of a thin current layer associated with the Kelvin-Helmholtz instability [22]. Exhaust jets from MMS1 and MMS2 were reported as evidence of reconnection. This letter focuses on the observations of MMS3 and MMS4. The mission and its instruments are described in several articles [14, 23-27].

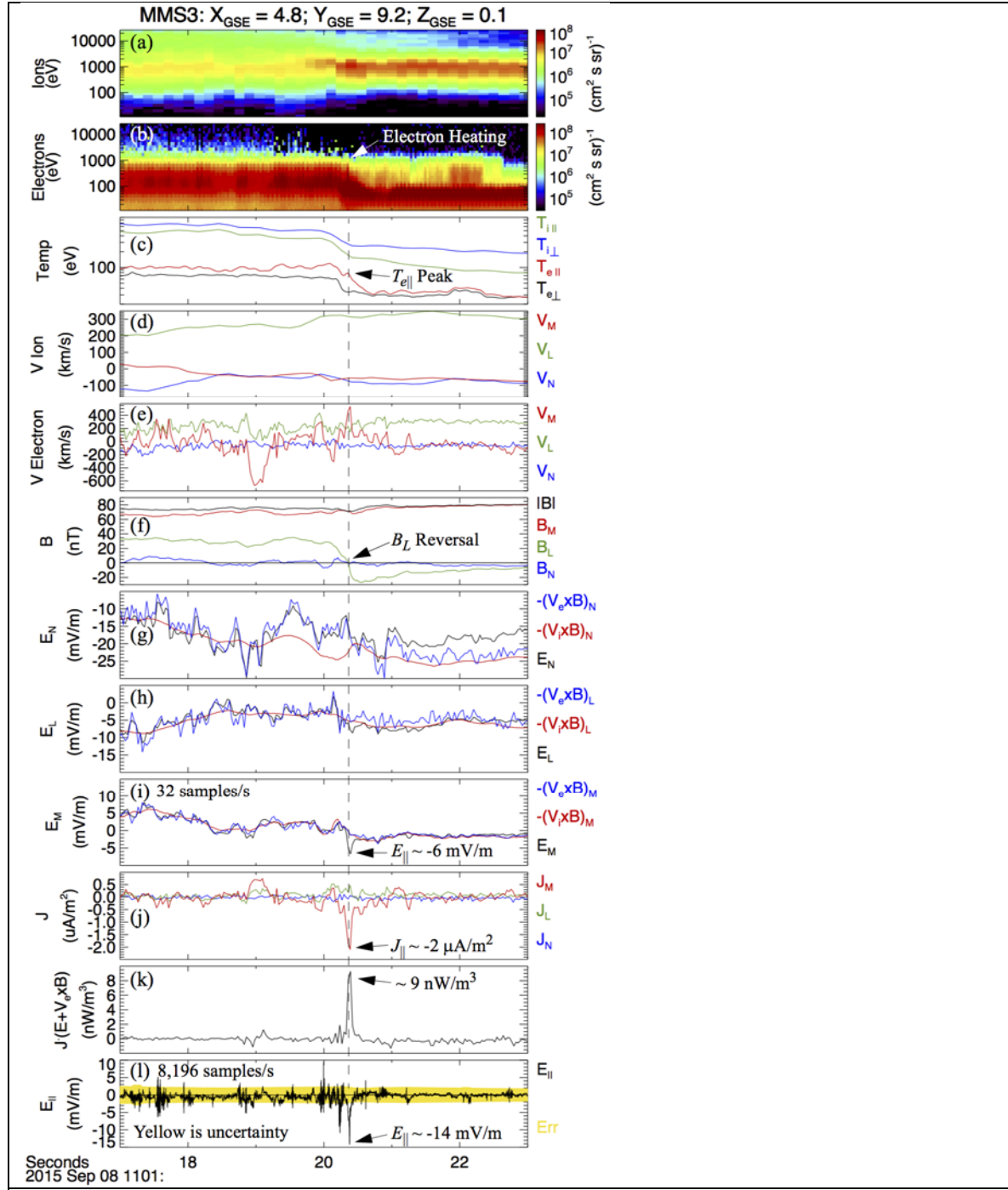


Figure 1. MMS3 observations that suggest an encounter with a large guide field EDR. (a,b) The differential ion and electron energy fluxes as a function of energy (vertical axis) and time. (c) T_i and T_e . (d) V_i . (e) V_e . (f) The magnetic field. (g-i) Measured E (black), $-V_i \times B$ (red), $-V_e \times B$ (blue). (j) $J = ne(V_i - V_e)$. (k) $J \cdot (E + V_e \times B)$. (l) $E_{||}$ measured at 8,192 samples/s. *LMN* coordinates are described in the text. The vertical dashed line marks 11:01:20.37 UT.

The top two panels of Figure 1, (a) and (b), display the ion and electron differential energy flux (color) as a function of energy (vertical axis) and time [27]. The electron distributions are at a cadence of 30 ms whereas the ion distributions have a cadence of 150 ms. Panel (c) plots the parallel and perpendicular values of the ion and electron temperatures (T_i and T_e). At the beginning of the plot until $\sim 11:01:20$ UT, MMS3 is in the magnetosphere. T_i is ~ 500 eV and T_e is ~ 100 eV. At $\sim 11:01:20$ UT, T_i lowers to < 200 eV and $T_{e\perp}$ noticeably reduces, indicating that MMS3 is detecting magnetosheath plasma. Of importance, there is a discernable peak in $T_{e\parallel}$ at $\sim 11:01:20.37$ UT (Panel c) that is apparent in Panel (b) as well (see arrow).

Panels (d) and (e) display the ion velocity (V_i) and the electron velocity (V_e) in a color-coded coordinate system labeled L , M , and N (see right side of plot). Panel (f) plots \mathbf{B} in the same coordinate system. The L direction, which represents the reconnecting \mathbf{B} , is derived as the direction of highest variance in \mathbf{B} (after linear detrending of $|\mathbf{B}|$) over a one second interval surrounding a local minimum in $|\mathbf{B}|$ at $\sim 11:01:20.37$ UT.

The minimum variance direction, however, cannot be determined with certainty as two eigenvalues are nearly identical. The M and N directions are chosen so that $B_N = 0$ at $\sim 11:01:20.37$ UT when $B_L = 0$ and when there is a local minimum in $|\mathbf{B}|$. Thus, the M direction lies in the current sheet and the N direction is normal to the current sheet. This choice of the M direction also minimizes $|B_N|$ over the time interval of Figure (1). This choice of M and N presumes a planar current sheet at $\sim 11:01:20.37$ UT. The directions L and N in Geocentric Solar Ecliptic (GSE) coordinates are indicated in Figure (2).

Figure 1d indicates a strong plasma flow of ~ -100 km/s in N and ~ 300 km/s in L . The plasma density at $\sim 11:01:20.37$ UT is ~ 20 cm $^{-3}$ yielding $\lambda_e \sim 1.7$ km. Roughly, 5 ms in time corresponds to traversing one λ_e in space and, correspondingly, ~ 250 ms in time corresponds to one ion skin depth ($\lambda_i \sim 75$ km).

Figures (1g, 1h, and 1i) show the three components of \mathbf{E} (E_N , E_L , and E_M , respectively). The black traces are measurements from the double probe electric field instrument [24, 25] at 32 samples/s. During this period, the uncertainty in the baseline (zero level) of \mathbf{E} is approximately ± 2 mV/m since a payload potential neutralizer was active [24]. \mathbf{E} and $(-\mathbf{V}_e \times \mathbf{B})$ are in good agreement for most of the region, except in the N direction after $\sim 11:01:21$ UT (Figure 1g). The E_N and/or $(-\mathbf{V}_e \times \mathbf{B})_N$ baselines can change as the plasma conditions change, particularly in the sunward direction (N is close to sunward), so the difference between E_N and $(-\mathbf{V}_e \times \mathbf{B})_N$ after $\sim 11:01:21$ UT is attributed to a baseline drift. However, the behavior of $(-\mathbf{V}_i \times \mathbf{B})$ distinctly differs from \mathbf{E} suggesting that MMS3 is in an ion diffusion region.

The short-duration difference between E_M and $(-\mathbf{V}_e \times \mathbf{B})_M$ at $\sim 11:01:20.37$ UT (Figure 1i), however, is significant. At this time \mathbf{B} is entirely in the M direction, so E_M represents E_{\parallel} , which is plotted with uncertainties in Figure (1l). The higher sampling rate in Figure (1l) reveals that the amplitude of E_{\parallel} is larger (~ 14 mV/m) and has a shorter time duration (~ 25 ms) than inferred from Figure (1i). The significant peak in J_M (Figure 1j) combined with the parallel electric field (Figure 1i) results in significant dissipation ($\mathbf{J} \cdot (\mathbf{E} + \mathbf{V}_e \times \mathbf{B})$, Figure 1k).

Figure (2) combines the measured \mathbf{B} , V_i , and time delays of the current sheet crossings of the four MMS spacecraft to reconstruct a plausible interpretation of the event in Figure 1. The MMS spacecraft are in a near tetrahedral formation with ~ 150 km separation. The plasma flow (V_i) is consistent between the MMS spacecraft indicating a stable current sheet. MMS1 and MMS2 cross the current sheet at a significant distance (> 150 km) in L from the location that MMS3 and MMS4 cross the current sheet. MMS1 and MMS2 detected exhaust jets coming from the

direction that MMS3 and MMS4 cross the current sheet [22]. Interestingly MMS4 is nearly directly behind MMS3 along the spacecraft trajectories (within ~ 28 km along L), so it crossed the current sheet at nearly the same location as MMS3. MMS3 and MMS4 do not detect jets, indicating that they were nearer to the X-line.

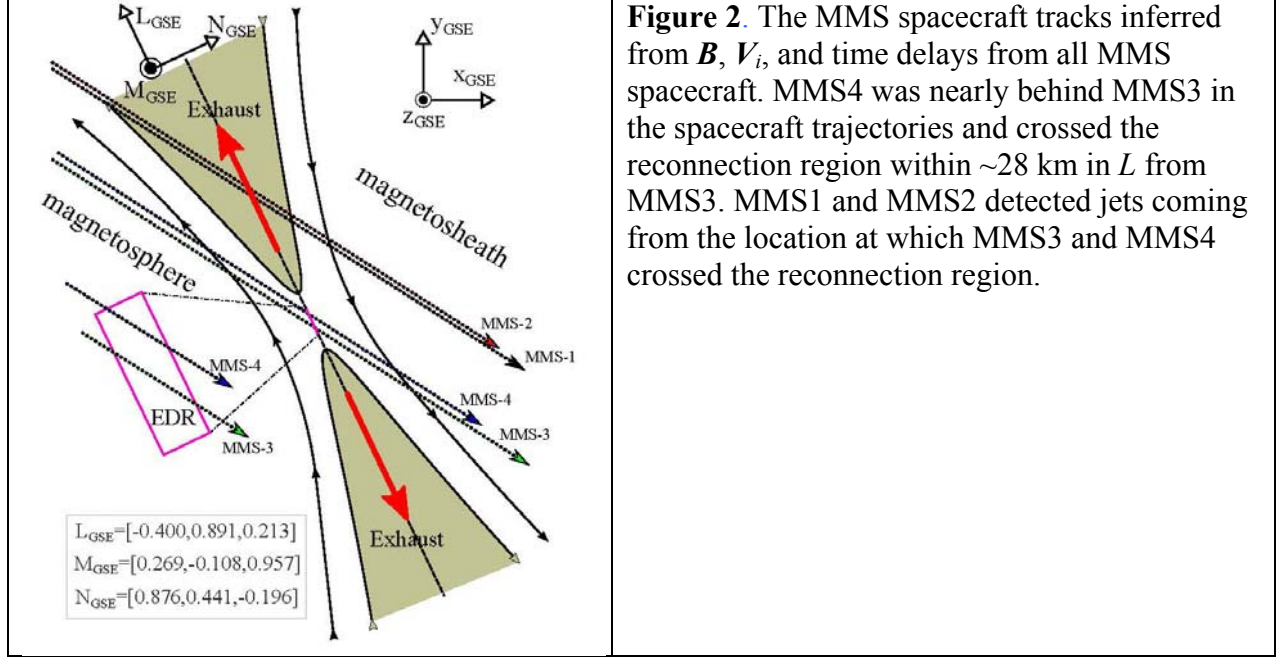
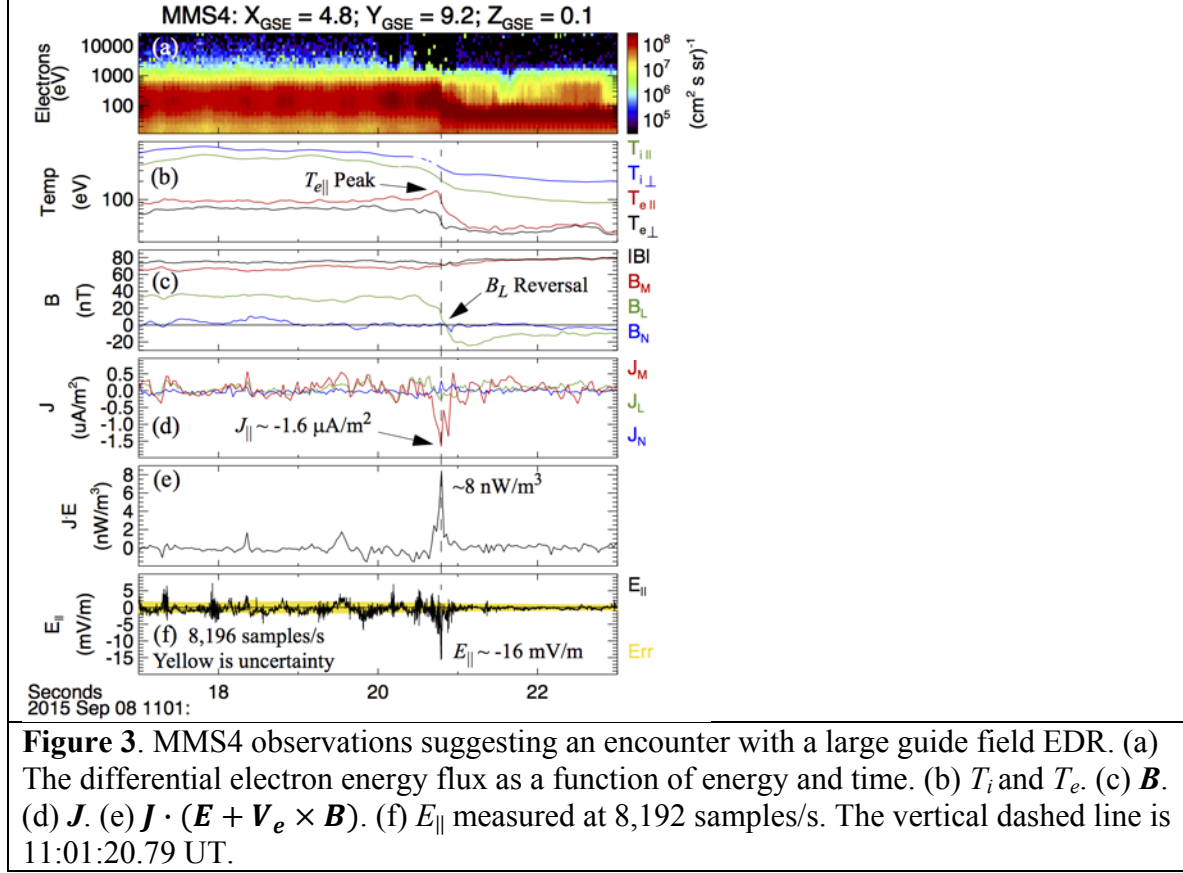


Figure (3) displays a subset of observations from MMS4, which crossed the current sheet at nearly the same location as MMS3's crossing. The format of Figure 3 is otherwise identical to that of Figure 1. The L , M , and N directions are those used in Figure 1. Many of the MMS4 observations are remarkably similar to those made by MMS3, but delayed by ~ 0.42 s, as determined by the peaks in E_{\parallel} .

Figure (3a) displays the electron differential energy flux and Figure (3b) plots T_i and T_e . The peak in $T_{e\parallel}$ at $\sim 11:01:20.73$ UT (Figure 3b) occurs just before the dashed vertical line, which marks 11:01:20.79 UT. The time at which $B_L = 0$ (Figure 3c) is delayed; it occurs at 11:01:20:85 UT. The peak in J_M (Figure 3d), the peak in $\mathbf{J} \cdot (\mathbf{E} + \mathbf{V}_e \times \mathbf{B})$, and the peak in E_{\parallel} are nearly simultaneous as indicated by the dashed line. The time differences between the peak in $T_{e\parallel}$, $B_L = 0$, and the peak in E_{\parallel} suggest that MMS4 may not have crossed the center of the EDR. The amplitude of E_{\parallel} from MMS4 is similar to that measured by MMS3, but the duration is shorter (~ 12 ms), supporting that MMS4 sampled a smaller portion of the EDR.



The observations in Figures (1) and (3) strongly suggest that MMS3 and MMS4 sampled the EDR of a large guide field reconnection event. The most persuasive evidence comes from the E_{\parallel} observations (Figures 1f and 3f), which appear to endure at least for the 0.42 s between successive crossings of MMS3 and MMS4. A finite E_{\parallel} is a necessary condition for magnetic topological change for reconnection with a guide field [28, 29]. In addition, observations of strong E_{\parallel} have been associated with secondary reconnection [30], that is, untangling newly reconnected magnetic fields. The individual probes of the axial double probe instrument [24] are separated by ~ 30 m. The individual probe signals of the E_{\parallel} peaks on MMS3 and on MMS4 show no detectable time delay (< 100 μ s), which is consistent with a crossing of an enduring E_{\parallel} structure at a velocity nearly perpendicular to \mathbf{B} .

The MMS3 (Figure 1) and MMS4 (Figure 3) spacecraft show, within error, nearly simultaneous occurrences of the E_{\parallel} peak, the peak in J_M , and a dissipative peak in $\mathbf{J} \cdot (\mathbf{E} + \mathbf{V}_e \times \mathbf{B})$. Dissipation is a feature of, albeit not unique to, the EDR of magnetic reconnection. On MMS3, the $B_L = 0$ (Figure 1f) occurrence is simultaneous with the E_{\parallel} peak. The peak in $T_{e\parallel}$ (Figure 1c) and a discernable change in the electron energy flux (Figure 1b) also are nearly simultaneous. These observations strongly suggest that MMS3 passed through the EDR.

The time difference between the peak in E_{\parallel} (Figure 3f) and the peak in $T_{e\parallel}$ (Figure 3b) indicates that MMS4 may have passed at the edge of the EDR rather than the center [31]. The delay in the time that $B_L = 0$ and the time of the peak in E_{\parallel} , however, can be partly attributed to the choice of the L , M , and N coordinate system, which is based on the MMS3 magnetic field. This

delay is reduced, but not entirely eliminated, if the L , M , and N coordinate system is based on MMS4 magnetic field.

III. ELECTRON DISTRIBUTIONS

The MMS3 and MMS4 observations afford an opportunity to study electron distributions within the EDR of large guide field reconnection. However, the speed at which the MMS3 and MMS4 spacecraft passed through the current sheet yield a dwell time of ~ 34 ms in an EDR of $2 \lambda_e \times 20 \lambda_e$ in size, enough time for only one electron distribution observation, which are compiled in 30 ms. Nonetheless, these observations may give insight to the physical processes of the EDR.

Figure (4a) displays full 2D electron pitch angle distributions measured by MMS3 60 ms prior to the peak in E_{\parallel} and $T_{e\parallel}$ (bottom semi-circle) and the 30 ms measurement essentially coincident with those peaks at 11:01:20.355 UT (top semi-circle). Pitch angle values are shown around the perimeter. The top distribution has been significantly heated in the field-parallel direction. This heating is better exemplified in Figure (4b), which shows cuts of the pitch angle distributions along (solid) and across (dashed) \mathbf{B} . The green and red traces correspond to the two distributions in Figure (4a), while the black one is 1/3rd of a second earlier and the blue one half a second later than the peak. These show the general vertical increase in the sharp shoulder in the anti-parallel direction and an increase in the parallel direction consistent with acceleration by E_{\parallel} (see arrow). The perpendicular direction does not participate in any significant variation throughout the main period of interest.

We have investigated the gyrotropy of the distributions by calculating the standard deviation of 16 individual azimuthal slices perpendicular to \mathbf{B} that are averaged to calculate the pitch angle distributions. This variation is typically $< 10\%$ below energies of 1keV and reaches at most 50% at isolated small regions in phase space (cf. the systematic variations by an order of magnitude reported in the low guide-field case [17]).

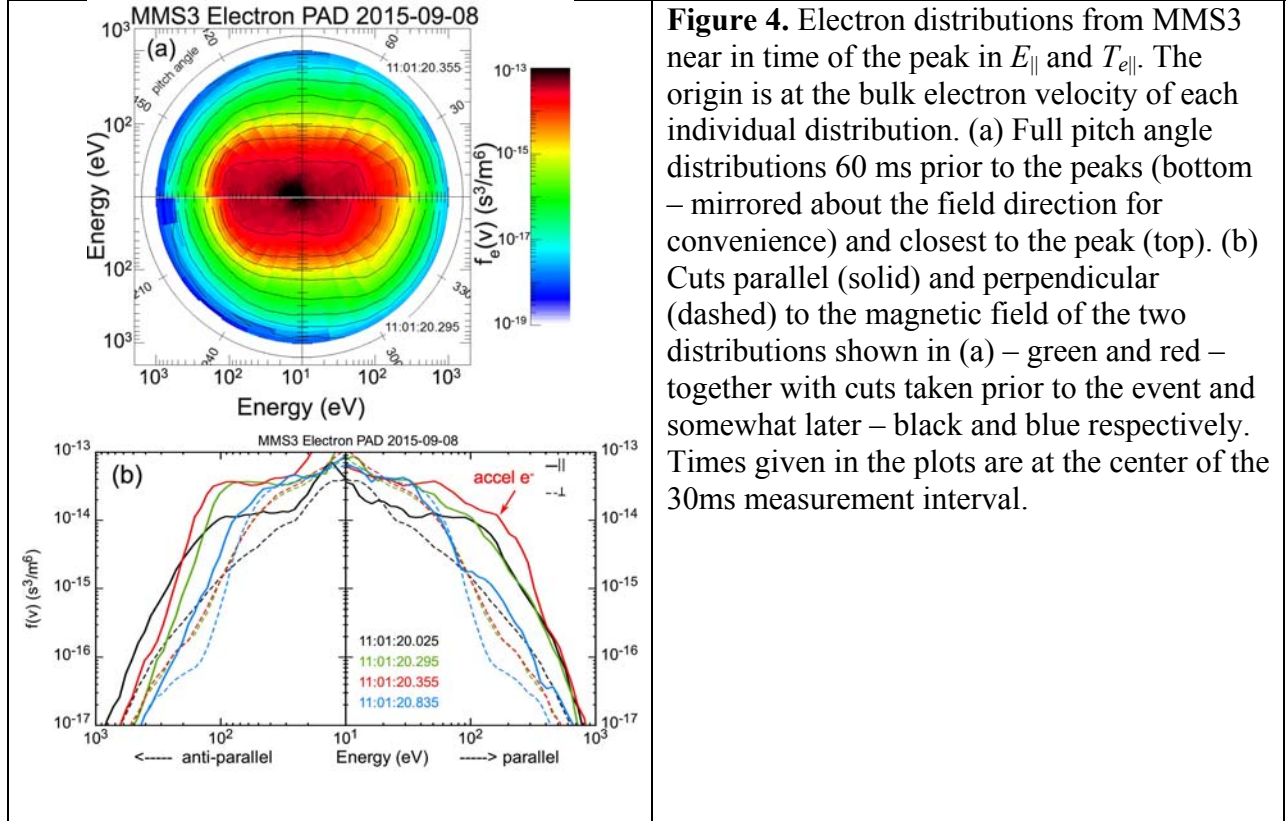
The electron pitch angle distributions from MMS4 (not shown) display similar characteristics leading up to the maximum in $T_{e\parallel}$ which occurs just prior to that in E_{\parallel} as described above. In particular, the heating is confined to the parallel stretching of $f(\mathbf{v})$, although in this case the parallel direction also develops a sharp, elevated shoulder. Again there is no indication of significant agyrotropy.

IV. DISCUSSION AND CONCLUSIONS

The observations suggest that MMS3 and MMS4 observed the EDR of a large guide field magnetic reconnection event. MMS3 displays the most convincing observations. As B_L , the in-plane magnetic field, crosses zero (corresponding to a local $|\mathbf{B}|$ minimum), a significant E_{\parallel} emerges concurrent with a parallel current and $\mathbf{J} \cdot (\mathbf{E} + \mathbf{V}_e \times \mathbf{B})$ dissipation. Nearly simultaneously, a peak in $T_{e\parallel}$ is seen along with an enhanced ~ 100 eV electron population traveling parallel to \mathbf{B} . There is no indication of agyrotropy in the electron distributions. However, the time that MMS dwelled in the EDR is nearly that of the compilation time of an electron distribution, so interpretations based on electron distributions cannot be conclusive.

The remarkably similar observations by the MMS4 satellite, which passed through the current sheet at nearly identical location 0.42 s later, strongly support the hypothesis that the two satellites traveled through the EDR. Again, E_{\parallel} emerges concurrent with a parallel current and $\mathbf{J} \cdot (\mathbf{E} + \mathbf{V}_e \times \mathbf{B})$ dissipation near the time that the in plane magnetic field passes through zero.

The peak in $T_{e\parallel}$ is before the E_{\parallel} event, indicating that MMS4 was either offset from the center of the EDR [31] or that the X-line is not entirely parallel to the guide field. Both MMS3 and MMS4 observe E_{\parallel} with an amplitude that is significantly larger than expected [18]. Both MMS3 and MMS4 observe enhanced $T_{e\parallel}$, but no measureable agyrotropy. These observations suggest that E_{\parallel} of large guide field magnetic reconnection may be supported by a parallel gradient of the gyrotropic electron pressure, or by electron inertia, that is, direct acceleration of electrons.



ACKNOWLEDGEMENTS

This work was funded by the NASA MMS project. The authors recognize the tremendous effort in developing and operating the MMS spacecraft and instruments and sincerely thank all involved. SJS thanks the Leverhulme Trust for their award of a Research Fellowship. IRAP contribution to MMS was supported by CNES and CNRS.

REFERENCES

- [1] G. Paschmann, *et al.*, *Nature*, **282**, 243–246 (1979).
- [2] B. U. Ö. Sonnerup, *et al.*, *J. Geophys. Res.*, **86**, 10049–10067 (1981).
- [3] S. Masuda, T. Kosugi, H. Hara, S. Tsuneta, Y. Ogawara, *Nature*, **371**, 495–497 (1994).

- [4] F. S. Mozer, S. D. Bale, and T. D. Phan, *Phys. Rev. Lett.*, **89**, 015002 (2002).
- [5] P. Louarn, *et al.*, *Geophys. Res. Lett.*, **31**, L19805 (2004).
- [6] J. T. Gosling, R. M. Skoug, D. J. McComas, and C. W. Smith, *J. Geophys. Res.*, **110**, A01107 (2005)
- [7] T. D. Phan, J. F. Drake, M. A. Shay, F. S. Mozer, and J. P. Eastwood, *Phys. Rev. Lett.*, **99**, 255002 (2007).
- [8] G. Paschmann, M. Øieroset, and T. Phan, *Space Sci. Rev.*, **178** (2–4), 385–417 (2013).
- [9] D. A. Uzdensky, B. Cerutti, and M. C. Begelman, *Astrophys. J. Lett.*, **737**, L40 (2011).
- [10] J. Egedal, W. Fox, N. Katz, M. Porkolab, K. Reim, and E. Zhang, *Phys. Rev. Lett.*, **98**, 015003 (2007).
- [11] J. Birn, *et al.*, *J. Geophys. Res.*, **106**, 3715-3719 (2001).
- [12] J. L. Burch, and J. F. Drake, *Am. Sci.*, **97**, 392–399 (2009)
- [13] M. Hesse, T. Neukirch, K. Schindler, M. Kuznetsova, and S. Zenitani, *Space Sci. Rev.*, **160**, 3–23 (2011).
- [14] J. L. Burch, T. E. Moore, R. B. Torbert, and B. L. Giles, *Space Sci. Rev.*, **199**, 5-21 (2016).
- [15] J. R. Shuster, L.-J. Chen, M. Hesse, M. R. Argall, W. Daughton, R. B. Torbert, and N. Bessho, *Geophys. Res. Lett.*, **42**, 2586–2593 (2015).
- [16] L.-J. Chen, M. Hesse, S. Wang, N. Bessho, and W. Daughton, *Geophys. Res. Lett.*, **43**, 068243, (2016).
- [17] J. L. Burch, *et al.*, *Science*, doi:10.1126/science.aaf2939, (2016).
- [18] M. Hesse, *et al.*, *Geophys. Res. Lett.*, **43**, 069373 (2016).
- [19] P. Ricci, J. U. Brackbill, W. Daughton, and G. Lapenta, *Phys. Plasmas*, **11**, 4102 (2004).
- [20] P. L. Pritchett, and F. V. Coroniti, *J. Geophys. Res.*, **109**, A10220 (2004).
- [21] M. TenBarge, W. Daughton, H. Karimabadi, G. G. Howes, and W. Dorland, *Phys. Plasmas* **21**, 020708 (2014).
- [22] S. Eriksson, *et al.*, *Geophys. Res. Lett.*, **43**, 068783 (2016).
- [23] R. B. Torbert, *et al.*, *Space Sci. Rev.*, **199**, 105-135 (2016).
- [24] R. E. Ergun, *et al.*, *Space Sci. Rev.*, **199**, 167-188 (2016).
- [25] P.-A. Lindqvist, *et al.*, *Space Sci. Rev.*, **199**, 137-165 (2016).
- [26] C. T. Russell, *et al.*, *Space Sci. Rev.*, **199**, 189-256 (2016).
- [27] C. Pollock, *et al.*, *Space Sci. Rev.*, **199**, 331-406 (2016).
- [28] M. Hesse, and K. Schindler, *J. Geophys. Res.*, **93**(A6), 5559-5567 (1988).
- [29] M. Hesse, T. Forbes, and J. Birn, *Astrophys. J.*, **631**, 1227 (2005).
- [30] R. E. Ergun, *et al.*, *Phys. Rev. Lett.*, *in press* (2016).
- [31] J. F. Drake, M. A. Shay, W. Thongthai, and M. Swisdak, *Phys. Rev. Lett.*, **94**, 095001 (2005).